Evolution of wave packets in quasi-one-dimensional and one-dimensional random media: Diffusion versus localization

F. M. Izrailev,[1,2,*] T. Kottos,[2] A. Politi,[3] and G. P. Tsironis[2]
[1]*Budker Institute of Nuclear Physics, 630090 Novosibirsk, Russia*
[2]*Department of Physics, University of Crete and Research Center of Crete, P.O. Box 2208, 71003 Heraklion-Crete, Greece*
[3]*Istituto Nazionale di Ottica, 50125 Firenze, Italy*
and INFN, Firenze, Italy
(Received 8 November 1996; revised manuscript received 17 January 1997)

We study numerically the evolution of wave packets in quasi-one-dimensional random systems described by a tight-binding Hamiltonian with long-range random interactions. Results are presented for the scaling properties of the width of packets in three time regimes: ballistic, diffusive, and localized. Particular attention is given to the fluctuations of packet widths in both the diffusive and localized regime. Scaling properties of the steady-state distribution are also analyzed and compared with a theoretical expression borrowed from the one-dimensional Anderson theory. Analogies and differences with the kicked rotator model and the one-dimensional localization are discussed. [S1063-651X(97)11603-8]

PACS number(s): 05.45.+b, 71.55.Jv

I. INTRODUCTION

The main approach to a statistical description of the spectra in complex quantum systems originates from the pioneering works of Wigner (see in [1]), who conjectured that random matrices could represent the simplest meaningful model for studying heavy nuclei. Currently, random matrix theory (RMT) has become a very effective tool in a large variety of physical applications. Until recently the matrices in this theory were assumed to be homogeneous, i.e., all matrix elements were taken to have identical statistics. This simplification is mainly dictated by mathematical reasons since the corresponding ensembles of random matrices are rotational invariant, a property that simplifies the theoretical analysis.

For a long time, the RMT had no concrete physical basis, in the sense that conditions for its applicability were not specified. It was believed that the systems under consideration had to be extremely complex in order to have a good agreement with the predictions of the RMT [1–3]. The situation has changed with the progress of the so-called quantum chaos theory which deals with dynamical Hamiltonian systems exhibiting chaotic motion in the classical limit. One of the main results of this theory is that in the extreme case, when classical motion is strongly chaotic and no influence of quantum localization is taken into account, statistical properties of both spectra and eigenfunctions are well described by the RMT. This statement has been thoroughly studied and confirmed both for autonomous systems, such as chaotic billiards [4], and for time-dependent models, such as the kicked rotator model (KR) [5,6] and the kicked tops [7]. Moreover, there are many physical examples where ''complexity'' of a quantum system is not maximal, but, nevertheless, a statistical description applies pretty well.

To describe the consequences of quantum localization in the presence of strong classical chaos, a new type of random matrices has been introduced when studying the KR [6,8]. The distinctive feature of these matrices is their bandlike structure, which is related to the finite range of interactions in a given basis. In a sense, the ensembles of band random matrices (BRM) can be regarded as an extension of the conventional random ensembles, since the latter are recovered by just setting the band size b equal to the matrix size N. Currently, the interest in BRM raised significantly due to their close relationship with quasi-one-dimensional (quasi-1D) models with random potentials [9], or 1D systems with long-range hoppings between neighboring sites. In the 1D interpretation, the band size b corresponds to the hopping range while in the quasi-1D case, it is associated with the number of transverse channels for electron wave propagation along a thin wire. Recent numerical and analytical studies of BRM (see [9,10] and references therein), led to numerous results regarding the structure of eigenstates. In particular, the localization length has been shown to depend only on the scaling parameter b^2/N, so as the statistical properties of the eigenstates that are directly related to the fluctuation properties of the conductance.

However, much less is known about the evolution of wave packets in models described by BRM. One should note that even in the ''simple'' case of Anderson-type models in 1D, only the short- and the long-time scales, corresponding to ballistic spread and saturation of the packet width, respectively, have been successfully studied [11]. In quasi-1D (or 1D with long-range hoppings) models, the picture is both more complicated and more interesting with respect to the Anderson case. Indeed, while the diffusion time scale is absent in 1D models of Anderson type, since the mean free path is of the order of the localization length, classical diffusion alters the ballistic spread in quasi-1D systems, before being eventually suppressed by localization effects.

In dynamical systems, the influence of strong localization on classical diffusion in momentum (or energy) space has been studied, in detail, in the framework of the KR. It was

*Electronic addresses: izrailev@ inp.nsk.su or izrailev@physics.spa.umn.edu

 © 1997 The American Physical Society

found that the time scale of the wave-packet spreading that is analogous to classical diffusion is much longer than the logarithmic time scale over which the complete correspondence between classical and quantum description holds [5,6,12,13]. The entire diffusive process, including the final saturation proved to exhibit remarkable scaling properties [6,13]. In particular, the diffusive time scale is proportional to the localization length of those eigenstates which are involved in the dynamics. In view of the analogies existing between dynamical and Anderson-type localization, the results obtained in the study of wave-packet evolution in the KR will represent the touchstone for the present investigation of packet dynamics in quasi-1D disordered models. However, because of the existence of basic differences as well (see Refs. [6,13–16]), it is not presently clear to what extent the similarity between dynamical and disordered systems can be pushed forward.

In this paper we extend a previous study [17] of initially δ-like wave packets in a quasi-1D geometry, with particular attention to their width and fluctuations on different time scales. We show that the scaling ansatz for the temporal scale has to be modified with respect to Ref. [17] in order to guarantee a convincing overlap of the results obtained for different bandwidths b, also presenting an argument to justify this new choice.

The paper is structured in the following way. In Sec. II, the model is introduced and discussed together with the main properties of spectra and eigenstates of BRM. In Sec. III both ballistic and diffusive time scales are analyzed and the scaling properties of packets in terms of bandwidth b are established. The effect of noise in the destruction of coherence is also briefly discussed. Section III terminates with the results for the suppression of classical diffusion due to the localization of eigenstates. In Sec. IV, we focus on the problem of fluctuations of the shape of packets both for the diffusive and relaxation time scales. In Sec. V, a phenomenological description of the asymptotic shape of the packets is given, based on results for the 1D Anderson model. Moreover, fluctuations along the asymptotic profile of packets are studied. The conclusions are summarized in Sec. VI.

II. BAND RANDOM MATRICES: MAIN PROPERTIES

A. Definitions and applications

Since its birth, random matrix theory has been mainly dealing with statistical properties of ''full'' random matrices, for which all matrix elements are independent and distributed according to the same law. In physical applications this implies that interactions are assumed to be so strong and complex that no other parameter, apart from the symmetry of matrices, is to be taken into account. As a result, such matrices are associated with the extreme case of maximal chaos which is known to appear in various physical systems, such as heavy nuclei, atoms, metallic clusters, etc. Furthermore, full random matrices represent a good model for the description of local statistical properties of spectra and eigenstates in some range of the energy spectrum, typically, in the semiclassical region.

On the other hand, the conventional RMT is both unable to describe important phenomena such as localization of eigenstates, and to characterize the spectra of physical systems influenced by strong localization effects. For this reason, much attention has been recently paid to the so-called band random matrices, which are characterized by the free parameter b defining the effective band width of a Hamiltonian. Such random matrices with elements decaying away from the main diagonal, appear to provide more realistic models for the Hamiltonian of ''complex'' quantum systems (see, e.g., [9,10] and references therein). The simplest type of BRM is given by matrices H_{nm} with zero elements outside the band ($|n-m|>b$), while inside the band ($|n-m|\leqslant b$), matrix elements are assumed to be independent and distributed according to a Gaussian law,

$$\mathcal{P}(H_{nm})=\frac{1}{\sigma_{nm}\sqrt{2\pi}}\exp(-H_{nm}^2/2\sigma_{nm}^2),$$

$$\sigma_{nm}^2\equiv\langle H_{nm}^2\rangle=\frac{\sigma_0^2}{2}(1+\delta_{nm}), \tag{1}$$

where δ_{nm} is the Kronecker symbol and $\sigma_0^2=2$, implying that the variance of the off-diagonal matrix elements are equal to 1. The BRM ensemble can be regarded as a generalization of the standard Gaussian orthogonal ensemble as the former reduces to the latter when $b=N$. Analogous generalizations can be introduced for the unitary and symplectic ensembles of band random matrices [9].

The limit case $b=0$ corresponds to diagonal matrices, while $b=1$ corresponds to tridiagonal Hamiltonians with both diagonal and off-diagonal disorder. The latter case is well known in the physics of disordered media; the main properties of such matrices are relatively well understood. The general case of BRM, where the variance of the matrix elements decreases with the distance from the main diagonal, introduced in [18], is also amenable to an analytic treatment. They are not, strictly speaking band matrices, but an effective band size b can be defined from the shape of the envelope [19].

In what follows, we consider large values of $b\gg 1$ and assume that $N\gg b^2$. The first condition implies a large number of nearby states coupled by the interaction. The second condition allows us to neglect finite size corrections arising from the finiteness of the samples.

Considerable interest towards the ensemble of BRM was stimulated by the investigation of the quantum behavior of periodically driven Hamiltonian systems. A paradigmatic system in this class is the kicked rotator model. Indeed, the unitary matrix U yielding the time evolution between two consecutive kicks has, in the angular momentum representation, a bandlike structure with an effective bandsize approximately equal to the strength k of the kicks. Outside the band, the matrix elements of U decrease extremely fast, while inside the band they can be treated as pseudorandom entries if the corresponding classical evolution is chaotic [6]. As a consequence, both spectra and eigenstates of BRM of the type (1) are expected to have statistical properties similar to those of the KR. A number of data substantiate this belief [9,10]. Recently, it has also been rigorously shown that the BRM model can be reduced to the more general nonlinear σ model [18]. As a consequence, BRM turn out to play an important role in the understanding of quasi-1D disordered media.

The above relationships gave a boost to the investigations of statistical properties of eigenstates and eigenvalues of BRM as they also allow us a better understanding of the properties of the KR, as well as of quasi-1D and 1D models with long-range random interactions.

B. Density of states and structure of eigenstates

As was first numerically shown in [20] and later analytically proved in [18], the density of states $\rho(E)$ for infinite BRM ($N\to\infty$) obeys the semicircle law

$$\rho(E)=\frac{1}{4\pi b v^2}\sqrt{8bv^2-E^2};\quad |E|\leqslant R_0=v\sqrt{8b}, \tag{2}$$

with $\rho(E)=0$ for $|E|>R_0$. The parameter v is just the standard deviation of the distribution of off-diagonal elements, $v^2=\langle H_{nm}^2\rangle=\sigma_0^2/2$; it does not influence the statistical properties of the spectra as well as the structure of the eigenstates, since it can be scaled out. For $b=N$, expression (2) reduces to the well known Wigner semicircle law derived in conventional RMT.

In infinite BRM, all eigenstates $\varphi_E(n)$ are known to be exponentially localized [9,10,20],

$$|\varphi_E(n)|\sim\exp\left(-\frac{|n-n_0|}{l_\infty(E)}\right),\quad n\to\pm\infty, \tag{3}$$

where n_0 is the ''center'' of an eigenfunction in the basis in which the random matrices have been defined. The quantity $l_\infty(E)$ is the localization length defined as the inverse of the asymptotic spatial decay rate of the amplitude of the corresponding eigenfunction. Numerically, $l_\infty(E)$ can be determined by implementing the transfer matrix method. It is important to recall that the localization length l_∞ describes the decay of the eigenfunction only in the tail and not in the central region of size $\approx b^2$. This region is characterized by an effective number $l\sim l_\infty$ of ''principal components'' which are usually defined in terms of the inverse participation ratio and of the so-called entropic localization length l_H (see [6,9] for details).

In finite samples, one more parameter comes into play, the rank N of the matrices. In such a case, all relevant properties of spectra and eigenstates are parametrized by the ratio $\lambda=b^2/N$ [9,10]. Upon changing λ, one can accurately follow the transition from the completely localized ($\lambda\ll 1$) to the delocalized ($\lambda\gg 1$) regime. Numerous studies of the BRM allowed us to unravel the dependence of the statistical properties of eigenfunctions on this scaling parameter. In particular, in finite bases of size N, all eigenstates are extended if $\lambda\gg 1$, and all their properties are very similar to those for the standard RMT. Our interest here is devoted to the opposite limit $\lambda\ll 1$ of very localized eigenstates where finite-size effects can be neglected. Based on the results obtained for the KR [6,20], it was predicted that the localization length l_∞ is proportional to b^2. A rigorous analysis [18] has confirmed this prediction and established the dependence $l_\infty\sim\rho^2 b^2$ of the localization length on the energy. In the case of BRM with a general envelope function $a(k)$ for matrix elements H_{nm},

$$l_\infty(E)=2\left[1-\left(\frac{E}{R_0}\right)^2\right]B;\quad B=\frac{\sum_{k=-\infty}^{\infty}a(k)\,k^2}{\left[\sum_{k=-\infty}^{\infty}a(k)\right]^2},$$

$$k=n-m, \tag{4}$$

where B is the second moment of the function $a(k)$. In case (1), i.e., for a sharp band of size b, one obtains $B=b^2/3$ and, thus,

$$l_\infty(E)=\frac{2}{3}\left[1-\left(\frac{E}{R_0}\right)^2\right]b^2. \tag{5}$$

At variance with the KR, the localization length of the eigenstates of BRM depends on the energy E.

C. Numerical procedure

Although considerable progress has been made in the description of the eigenstate structure (see [9,10] and references therein), the evolution of wave packets is still poorly understood even in the limit of infinite samples. The mathematical model we consider below is the time-dependent Schrödinger equation on a 1D lattice,

$$i\frac{dc_n(t)}{dt}=\sum_{m=n-b}^{n+b}H_{nm}c_m(t), \tag{6}$$

where $c_n(t)$ is the probability amplitude for an electron to be at site n and H_{nm} is a symmetric BRM of the type (1). Equation (6) has been integrated numerically using a finite-time step ($dt\simeq 10^{-3}-10^{-4}$) fourth order Runge-Kutta algorithm on a self-expanding lattice in order to eliminate finite-size effects [21]. Whenever the probability of finding the particle at the edges of the chain exceeded 10^{-15}, $10b$ new sites were added to each edge. The initial condition was taken to be a δ-like state located in the middle of the chain, i.e., $c_n(t=0)=\delta_{n,0}$. At each time step, the normalization condition for the total probability, $\Sigma_n|c_n(t)|^2=1$, was checked observing fluctuations smaller than 10^{-4}.

A further check of the accuracy of our calculations has been performed by reversing the time-axis direction after 2000 time units (for $b=10$). The difference between the initial probability distribution and that obtained after integrating for 2000+2000 units was found to be less than 10^{-13}. In all the cases discussed below, a large number of disorder realizations has been considered (more than 150) in order to get rid of sample-to-sample fluctuations.

III. DIFFUSION OF WAVE PACKETS

The time-evolution of a quantum wave packet in the lattice is naturally described by the mean-square displacement,

$$M(b,t)=\langle u(t)\rangle\equiv\left\langle\sum_m m^2|c_m(t)|^2\right\rangle, \tag{7}$$

where $\langle\cdots\rangle$ stands for the average over different realizations of the frozen disorder H_{nm}. The time dependence of

$M(b,t)$ provides a qualitative description of the dynamical regime: a power-law evolution $M(t)\sim t^{\nu}$, where $\nu<1$ corresponds to a subdiffusive behavior (hinting at a possible, eventual localization), $\nu=1$ corresponds to ordinary diffusion, while $\nu>1$ to superdiffusion ($\nu=2$ characterizes ballistic motion).

As mentioned above, BRM can be regarded as a good model for dynamical quantum systems such as the KR in the region of strong classical chaos. In the classical limit, this model exhibits an unbounded diffusion in angular momentum space if the kick strength exceeds some critical value. It was discovered that even in the deep semiclassical domain, quantum effects can suppress classical diffusion [5] giving rise to a phenomenon that is closely related to Anderson localization of a quantum particle in random potentials [22–24]. This effect of ''dynamical localization'' was claimed to be experimentally observed in the ionization of hydrogen subject to a monochromatic field [25]. A formal connection with a 1D tight-binding model has been found in [26], thus reviving a general interest for localization in one-dimensional systems.

We have investigated the behavior of $M(b,t)$ by numerically integrating Eq. (6) for different values of b. The results of our analysis have been compared with both theoretical predictions of the 1D Anderson model and numerical findings for the KR.

A. Ballistic time scale

The essential difference between periodic and disordered quantum lattice structures mostly lies in the localization properties of their electronic states. In the periodic case, all the states are perfectly extended Bloch waves, while in strongly disordered samples, the packets are asymptotically localized in time because of quantum interference effects. However, even in the latter case, there exists a ballistic regime, occurring on time scales of the order of the elastic scattering time t_b, i.e., the time for an electron to move by an amount corresponding to the mean free path l_m. In quasi-1D systems, l_m is known to be equal to the number of transverse channels.

In order to investigate the scaling behavior of the packet size with b, we have numerically integrated Eq. (6) for very short times $\sim t_b$ and different values of b in the range $b=20$–45. The behavior of the mean-square displacement $M(b,t)$ is reported in Fig. 1 with the scaling assumption

$$M(b,t)=b^2\widetilde{M}(t\sqrt{b}). \tag{8}$$

The very good data collapse confirms the scaling anzatz. Equation (8) can be understood by estimating the ballistic time scale t_b. Let us start by noticing that the leading contribution to the wave packet spreading over short-time scales comes from the $2b$ sites which are directly coupled with the site $n=0$ where the wave packet is concentrated at time $t=0$. By evaluating the Schrödinger equation and thereby determining $M(b,t)$, one obtains

$$M(b,t)=\sum_{n=-b}^{b} n^2|H_{n,0}|^2t^2\approx b^3t^2. \tag{9}$$

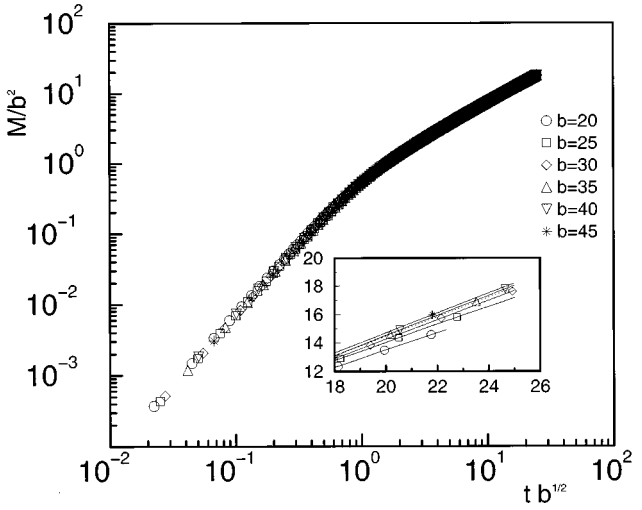

FIG. 1. Scaling behavior of $M(b,t)$ vs time in the ballistic time scale. The reported values of b are $b=20$, 25, 30, 35, 40, and 45. The inset shows the lost of scaling for $t>t_b$.

The above type of evolution terminates when the average width $\sqrt{M}$ of the packet becomes of the same order as the bandsize b, so that farther sites come into play. By substituting back in Eq. (9), one finds that the ballistic spread occurs on the time scale

$$t\leqslant t_b\approx\frac{1}{\sqrt{b}}. \tag{10}$$

Accordingly, the ballistic time scale shrinks to zero for increasing the interaction range b. Notice that the ballistic regime is entirely new with respect to the analogous problem in the KR where, at small times, an exponentially fast spread of the packet takes place.

B. Diffusive time scale

In 1D Anderson-type models, wave packet saturation starts immediately beyond the ballistic time scale, since the mean free path l_m and the localization length l_∞ are of the same order ($l_\infty\approx 2l_m$). Accordingly, no intermediate diffusive regime can be observed. In the case of a large bandsize $b\gg 1$, the localization length $l_\infty\sim b^2$ is much larger than the mean free path $l_m\sim b$, so that a diffusive time scale t_D appears. In order to estimate t_D, we shall follow the scaling arguments developed from the theory of quantum chaos where they have been successfully introduced to explain the well known ''quantum suppression of classical diffusion'' in the KR [12].

The first crucial observation is that the eigenfunctions $\varphi_E(n)$ are exponentially localized in the standard basis for all energy values E in the spectrum [consequently, there is a pure-point spectrum $\rho(E)$]. Let us proceed by noticing that an initial state $c_n(t=0)$ excites an effective, finite number N_{eff} of eigenstates with corresponding energies E_i. Accordingly, the spectrum of those eigenstates participating to the evolution of the packet is characterized by a mean level spacing $\Delta_{\text{eff}}\sim R_0/N_{\text{eff}}$ where $R_0^2=8bv^2$ is the radius of the semicircle, see Eq. (2).

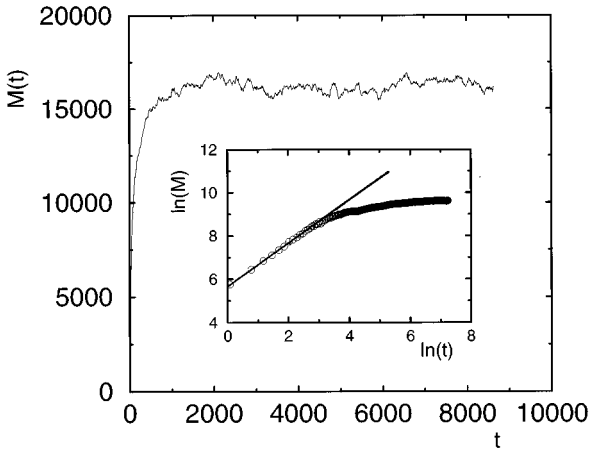

FIG. 2. An example of wave-packet diffusion beyond the ballistic time scale for $b=12$. The same curve is reported (in a doubly logarithmic plot) in the inset, magnifying the early stages of diffusion, to testify the linear behavior.

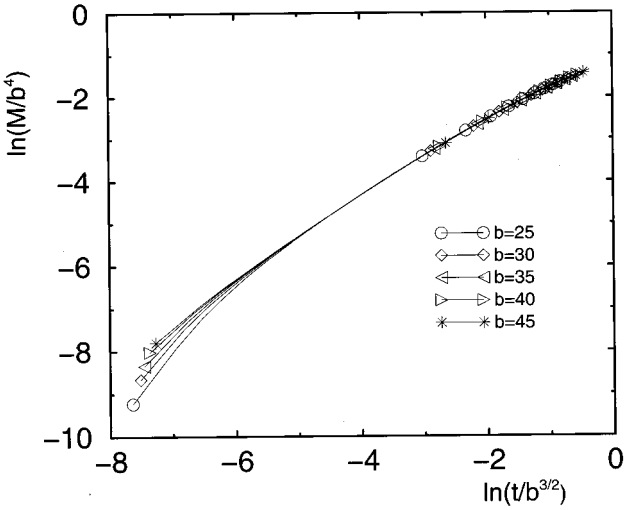

FIG. 3. Scaling of $M(b,t)$ vs time in the diffusive time scale. The reported values of b are $b=25$, 30, 35, 40, and 45.

Therefore, for times $t<1/\Delta_{\rm eff}$, the packet evolution does not ''feel'' the discreteness of the spectrum, which is resolved over longer time scales and eventually leads to localization. A typical evolution is reported in Fig. 2, where the dependence of the mean-square displacement $M(b,t)$ for $b=12$ is shown on a very large time scale. However, as long as $t_b \leqslant t \leqslant t_D$, with

$$t_D \approx N_{\rm eff}/R_0 \tag{11}$$

the motion of the particle is analogous to the standard (classical) diffusion. This means that $M \approx Dt$, where D is the diffusion constant and M can be interpreted as the square of the number of effectively excited, unperturbed states. This regime is clearly seen in the inset of Fig. 2, where the evolution of M is reported in a doubly logarithmic plot.

The quantity M reaches its maximal value $M_{\rm max}$ at $t \approx t_D$. The value $M_{\rm max}^{1/2}$ is of the same order as the total number $N_{\rm eff}$ of eigenstates that participate to the packet evolution. Let us finally notice that the packet width is asymptotically of the order of the localization length of the eigenfunctions, i.e., $N_{\rm eff} \sim l_\infty \sim b^2$ (the energy dependence is here irrelevant and can be dropped). Accordingly, the following scaling relations hold:

$$t_D \sim l_\infty/R_0, \quad D \sim l_\infty R_0, \tag{12}$$

where R_0 is the width of the spectrum. The second estimate in Eq. (12) corresponds to the well known relation between the localization length and the diffusion coefficient in the theory of disordered solids $l_\infty \approx \pi \rho D$, where ρ is the density of states (see, for example, [9]). Accordingly, Eq. (12) suggests the following scaling relation for the mean-square displacement $M(b,t)$

$$M(b,t) = b^4 \widetilde{M}(t/b^{3/2}). \tag{13}$$

The numerical results obtained for quite large values of the bandwidth ($b=25$, 30, 35, 40, and 45) are reported in Fig. 3 according to the above ansatz. The very good overlap indeed confirms the expected scaling dependence. There are only minor deviations at small times which are to be attributed to the crossover to the ballistic regime. Notice that the scaling factor of the temporal axis is different from the value conjectured in Ref. [17] ($t \to t/b^2$), on the basis of small b simulations.

Equation (12) seems to suggest that there is a substantial disagreement with the value of the diffusive time obtained in the KR model. However, this discrepancy is to be attributed to the choice of the time units adopted in model (1). Indeed, in dimensionless units, we recover the results obtained in the KR model, i.e.,

$$\widetilde{t}_D \equiv \frac{t_D}{1/R_0} \sim l_\infty, \quad \widetilde{D} \equiv D/R_0 \sim l_\infty. \tag{14}$$

C. Diffusion suppression and scaling properties

One of the most important peculiarities of the time evolution of wave packets in 1D and quasi-1D random potentials is the saturation of the width M for $t \to \infty$. In analogy with the evolution of wave packets in the KR [6] and from the localization properties of the stationary problem (the localization length grows as b^2), one expects that for $b \gg 1$ the limiting value $M_\infty(b)$ grows as b^4. In order to confirm this prediction, we have performed detailed numerical experiments, in the range $b=4$–12. The asymptotic value $M_\infty(b)$ has been accurately determined by averaging $M(b,t)$ over a long time after an initial transient. From our data we have found that the dependence of M_∞ on b is slightly slower than expected, $M_\infty \sim b^\alpha$ with $\alpha \approx 3.87 \pm 0.02$. This anomalous behavior is presumably to be attributed to the presence of finite band-size corrections which are not negligible in the range of b values that has been numerically investigated ($b \leqslant 12$). Our results are reported in Fig. 4, where $M(b,t)$ and t are divided by the asymptotic value M_∞ and $M_\infty^{3/8}$, respectively. While the scaling ansatz for M follows straightforwardly from the detailed knowledge of the localization properties, the rescaling of time axis follows from Eq. (13) (we have preferred to

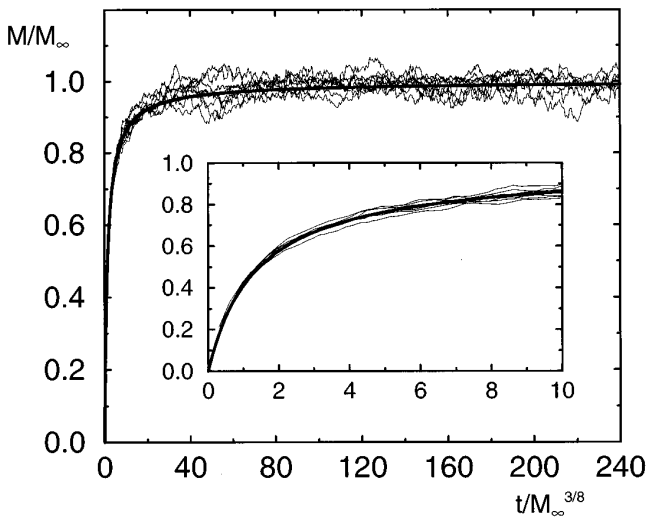

FIG. 4. Mean-square displacement M for $b=4-12$. The smooth curve corresponds to the phenomenological expression (18). In the inset the same quantities are shown for shorter times.

scale the data with reference to M_∞, rather than to b as the former choice appears to better account for finite-''size'' corrections).

Anyway, the nontrivial evolution during the late stages of the diffusive regime confirmed by a direct investigation. Since generic properties of eigenstates in quasi-1D models have been found to be similar to those of strictly 1D disordered models [9], it is natural to expect that the similarity extends to the dynamics of wave packets as well. However, even in 1D geometry, the analytical treatment is very difficult. Analytical results are available only in the two opposite regimes, $t \ll 1$ and $t \gg t_D$. For example, the asymptotic dependence of the mean-squared displacement $\langle u(t)\rangle \equiv \langle x^2(t)\rangle$ of packets in the long-time limit is given by [11],

$$\langle u(t)\rangle \simeq a_0 l_m^2 \left(1 - \frac{\ln(t/2t_m)}{t/2t_m}\right), \quad t \gg t_m \tag{15}$$

where l_m and t_m are the mean free path and the corresponding time between consecutive back scattering processes. This estimate is based on the expression for the quantum diffusion coefficient obtained in [24]. The logarithmic singularity in Eq. (15) follows from resonant transitions occurring between pairs of the so-called Mott states [27,28]. Such states have a peculiar structure characterized by two humps lying at a distance much larger than their effective width. Since Mott states appear in pairs, the corresponding energies are very close to each other and this results in a resonant tunneling over large distances. The influence of Mott states on electronic properties of disordered 1D models has been studied in [29], where the clustering of energy levels was discovered and attributed to these states.

The effect of these states has been included in the study of the long-time behavior of wave packets in the KR [30], where an expression similar to Eq. (15) has been introduced to describe the evolution of the mean-square displacement $M(t)$ in the momentum representation,

$$\widetilde{R} \equiv \frac{dM}{dt} \sim \frac{D^2 \ln[t/(2D)]}{[t/(2D)]^2}, \quad t \gg 2D \tag{16}$$

where D is the classical diffusion coefficient. Numerical data seems to confirm the expectations [Eq. (16)], although the presence of very large fluctuations prevent us from drawing a convincing conclusion. Despite the better statistics of our data, the presence of the logarithmic correction cannot be definitely assessed in BRM too.

Another approach to the problem of quantum diffusion in the presence of strong localization has been recently suggested in [31] (see further developments in [14]): it is essentially based on a phenomenological diffusion equation for Green's function, which takes into account backward scattering. At large times, the relaxation rate is given by [14]

$$\widetilde{R} \sim \frac{D^2 \ln^{3/2}[t/(2D)]}{(t/2D)^2}, \quad t \gg 2D \tag{17}$$

which differs from Eq. (16) by a further logarithmic factor. At the moment, all available numerical data for the KR do not allow us to draw a final conclusion in favor of either expression. In any case, let us again remark that the quantum localization in the KR is of a dynamical nature (there is no randomness in the model), so that it is not clear to what extent it is similar to the localization of Anderson type.

Instead of focusing on the question of the exact asymptotic dependence ($t \to \infty$) of the mean-square displacement $M(b,t)$, it is, for the time being, more useful to limit ourselves to provide an effective description of the wide time region that also includes the crossover from classical diffusion to complete saturation. In the absence of any theory, we make use of the phenomenological expression suggested in [32] (see also [6])

$$M(b,t) = M_\infty(b)\left(1 - \frac{1}{(1+t/t_D)^\beta}\right), \tag{18}$$

where M_∞, t_D, and β are the three independent parameters to be determined. The first one is obviously obtained from the asymptotic evolution, while the short-time classical diffusion (here, we neglect the ballistic time scale which is indeed negligible for large b) provides a further constraint to be fulfilled. In fact, for $t \ll t_D$, Eq. (18) reduces to

$$M(b,t) = \frac{\beta M_\infty}{t_D} t = Dt, \tag{19}$$

which allows us to express t_D in terms of the last unknown β which can be determined by fitting the global behavior of $M(b,t)$.

The main idea behind the phenomenological expression (18) is the repulsion of the energy levels participating in the evolution of the packet. As was previously discussed, the diffusion rate is proportional to the mean spectral density and it remains unchanged for $t \leqslant t_D$, according to the uncertainty principle. However, for $t \geqslant t_D$ it decreases, since the only eigenstates that continue to contribute (''operative eigenstates'') are those whose energy level spacing s satisfies the relation $s \leqslant t_D/t$. The relative number of such spacings

(hence, the relative diffusion rate) is given by the spacing distribution $p(s)$ for the operative eigenstates,

$$\frac{D(t)}{D} \sim \int_0^s p(s')ds' \sim s^{\beta+1} \sim \left(\frac{t_D}{t}\right)^{\beta+1}, \qquad (20)$$

where $t \gg t_D$ is assumed. The above time dependence for large times is the core of the phenomenological expression (18) (see details in [6,32]).

According to the above relation, the parameter β characterizes an effective repulsion between those eigenstates which are excited by the initial wave packet. It is clear that these eigenstates strongly overlap. As a result, the value of β can be expected to be quite close to 1. Although these arguments are no longer valid for very long times, when the level clustering [16,33] due to the influence of Mott states becomes important, Eq. (18) can still provide a sufficiently good description of the packet dynamics. Numerical experiments done for the KR [6,32] yield quite a small value of β ($\beta \approx 0.3$). This result, which is somehow contradictory with other studies (see the discussion in [31]), is probably due to the insufficiently long times considered in the simulations.

Our detailed numerical experiments with BRM, performed on a much longer time scale and with high statistics, reveal quite a good correspondence with the scaling dependence (18) (see Fig. 4). The best fit of Eq. (18) gives the following values: $\beta \approx 0.9$ and $t_D \simeq b^{1.5}$. Since the values of the band size b are not very large, the limiting value M_∞ has been purposely rescaled to the same level for the different b values. By neglecting the residual weak deviations from a perfect scaling, we obtain $D \approx 0.83 b^{2.5}$. The most important point of the above analysis is that the value of the repulsion parameter β is quite close to 1. This means that even for very large times close to the relaxation, the approximate power dependence $1/t^{0.9}$ for the difference $\Delta M = M_\infty(b) - M(b,t)$ mimics the correct dependence $\Delta M \sim \ln(t)/t$ [see Eq. (15)]. As a result, one can treat the scaling dependence (18) as a good description of both classical diffusion and its suppression due to strong localization of eigenstates.

The asymptotic localization of the wave packet is entirely a consequence of the frozen character of the disorder in the Hamiltonian. However, in reality, physical systems are also subjected to time-dependent noise (this is, for instance, the case of applications to nuclear physics [34]). In the KR, the influence of a time-dependent noise was discussed for the first time in [35] (see also the detailed investigation in [36]), finding that if the strength of the noise exceeds some critical value, then it destroys coherent effects of quantum localization and pure classical diffusion is recovered.

The addition of noise to the BRM provides an alternative method to determine the diffusion coefficient D from the direct computation of the linear growth of $M(b,t)$. It is first interesting to notice that the computation of D cannot be easily performed in practice without the presence of noise. The reason is that in the absence of a time-dependent noise, corrections to the linear behavior of $M(b,t)$ arise already at short times, thus preventing an accurate determination of the coefficient of the linear growth. In other words, coherent effects of quantum localization come into play even on the time scale of classical diffusion and this results in a rather smooth transition from classical diffusion to complete relaxation (see Fig. 4).

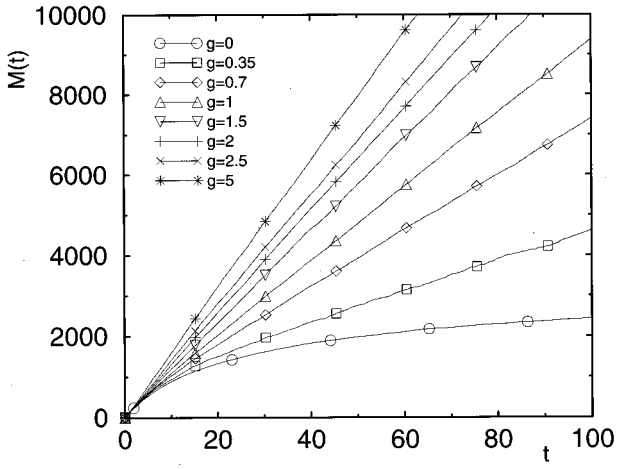

FIG. 5. Diffusion of packets with additional noise for $b=8$. The diffusive constant is determined from simulations performed for different noise strengths g^2.

In order to estimate the critical value of the noise strength g_{cr}^2 which completely destroys quantum coherence and leads to pure classical diffusion, one needs to compare the shift of levels induced by the additional noise, with the mean level spacing between operative eigenstates. Since the latter turns out to be proportional to $1/b^{1.5}$, one can see that if the shift $\Delta E \approx g^2 t_D$ is larger than $1/b^{1.5}$, localization will be completely destroyed. Accordingly, effects of quantum coherence should be observable only when the condition $g^2 \geqslant 1/b^3$ is satisfied. Our numerical simulations confirm this estimate: the data in Fig. 5, which refer to $b=8$, show that for $g=g_{cr}=5$ (in units of $b^{-1.5}$) we have $D/b^{2.5} \approx 0.86$ in good agreement with the value found from the fit of the scaling dependence given by Eq. (18). We would like to stress that diffusion due to the noise occurs also for $g<g_{cr}$; however, the rate of such diffusion is different from that given by the classical diffusion determined in the limit $b \to \infty$ (for details see, e.g., [36]).

IV. FLUCTUATIONS OF PACKET WIDTH

In any statistical process, the analysis of average quantities provides a limited description of the underlying properties. At least the variance should be considered in order to achieve a more complete characterization of the phenomenon of interest. In the present case, we shall consider the fluctuations of $M(b,t)$ in both the diffusive ($t_b \leqslant t \leqslant t_D$) and the relaxation ($t \geqslant t_D$) regime. The relevant quantity to be determined is the size of sample-to-sample fluctuations,

$$\Delta M(b,t) \equiv [\langle u(t)^2 \rangle - \langle u(t) \rangle^2]^{1/2}, \qquad (21)$$

where the brackets $\langle \cdots \rangle$ denote the average over different realizations of the Hamiltonian H_{nm}. A meaningful way to present the numerical data is through the relative amplitude $\mu \equiv \Delta M/M$ of the fluctuations. Its scaling properties with b are discussed in the Secs. IV A and IV B.

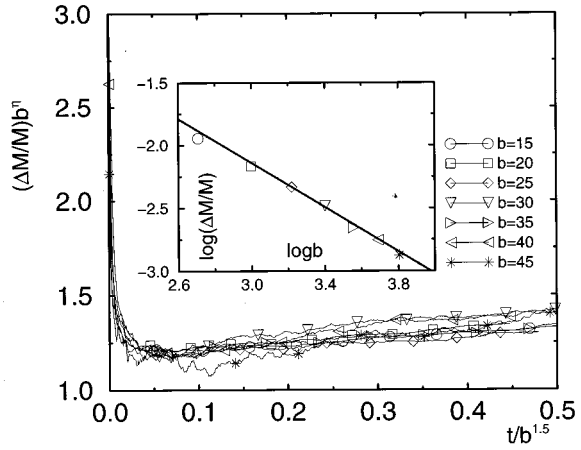

FIG. 6. Relative fluctuations on the diffusive time scale. The data is scaled according to Eq. (22). In the inset, a least-square fit for the same quantity and different b values is shown; the time is fixed, $t=0.5b^{1.5}$.

A. Diffusive time scale

As the diffusive time scale is relatively short, we have been able to determine μ for quite large b values (namely, $b\leqslant 45$), so that finite band-size corrections should be definitely negligible. In our numerical experiments, we have integrated Eq. (6) up to a time $t_m=b^{3/2}/2$ for more than 1000 realizations of the disorder. The results are reported in Fig. 6 under the scaling assumption

$$\mu(b,t)\approx b^{-\eta}\overline{\mu}(t/b^{1.5}). \tag{22}$$

By performing a least-square fit of $\ln\mu$ versus $\ln b$ at fixed time $t=b^{3/2}/2$, well inside the diffusive regime, we have estimated η which turns out to be approximately 0.9 ± 0.02 (see the inset in Fig. 6). One should notice the reasonable agreement with the value of the exponent recently obtained in the KR [37], $\eta\approx 1.0$. This scaling parameter has been conjectured to be related to the mesoscopic fluctuations of the diffusion coefficient [37]. However, the connection has not been entirely clarified.

B. Relaxation time scale

The next important issue concerns fluctuations around the so-called steady-state distribution of the wave packet in the asymptotic regime $t\gg t_D$. If one assumes that the steady-state distribution of $c_n(t\to\infty)$ is characterized by an ergodic spread of the packet over some finite size N_s, and if the components c_n are statistically independent, then

$$\mu\equiv\frac{\Delta M}{M}\approx\frac{1}{\sqrt{N_s}}. \tag{23}$$

Since the components c_n are directly related to the amplitudes of eigenstates and the latter are expected to be random on the scale of their localization length, one can conclude that $N_s\approx\langle l_\infty(b)\rangle\sim b^2$, i.e., $\mu\approx 1/b$. However, our numerical data in the range $b=4$–12 indicate that

$$\mu(t/b^{3/2})\approx\frac{1}{b^{\delta}}, \tag{24}$$

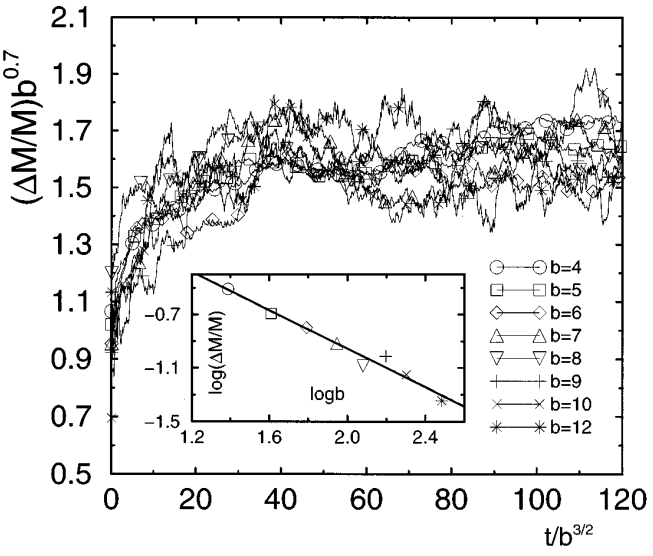

FIG. 7. Relative fluctuations in the saturation regime. The values of b are 4, 5, 6, 7, 8, 10, and 12. In the inset, a least square fitting is shown for the same quantity which now is averaged over time from $t=40b^{3/2}$ up to $t=250b^{3/2}$.

with $\delta\approx 0.7$ (see Fig. 7). A detailed study shows that when the value of δ is varied by ± 0.1, the superposition of the various curves on the plateau gets appreciably worse. As an additional check, we have performed a least-square fitting of μ versus b after averaging the curves over times $t>40b^{3/2}$. The fit presented in the inset of Fig. 7, confirms the value $\delta\approx 0.7\pm 0.01$. One should note that this value is in disagreement with the result found on the diffusive time scale for the factor η. This has to be attributed to the spatial structure of the Mott states (see below) appearing to control the evolution of the packet for times $t\gg t_D$. We would like to stress that the anomalous scaling described by Eq. (24), is in close agreement with the numerical data for the KR, where it has been observed that $\mu\sim b^{-\delta}$ with an anomalous exponent $\delta\approx 0.6$ [14]. Note that in the KR, larger values of the effective parameter b have been reached.

In Ref. [14] it was conjectured that the above anomalous scaling can be considered as an indication of the fractal structure of the quantum steady-state distribution $c_n(t\to\infty)$. More precisely, they argued that the asymptotic shape can be described by an ensemble of only $N_s\sim l_\infty^{0.6}$ statistically independent degrees of freedom (N_s being the number of ''channels'' where the amplitude of the wave packet is essentially different from zero). The same conjecture can be raised in the present case as well, although a direct check is an extremely hard task. Let us finally mention, that such an argument is compatible with the existence of Mott states which mainly participate at the structure of the steady state.

In order to better disentangle the question of fluctuations, we have also investigated the temporal behavior of $M(b,t)$. The main motivation for this study is the comparison between sample-to-sample and temporal fluctuations for a typical realization of the disorder. In practice, we have integrated the Schrödinger equation for a time up to $t=250b^{3/2}$, discarding an initial transient time $t<t_0=40b^{3/2}$ [which is sufficiently long for $M(t)$ to saturate]. The Fourier power spectrum $|U(\omega)|^2$ of $u(t)$ [let us recall that $M(t)=\langle u(t)\rangle$] has

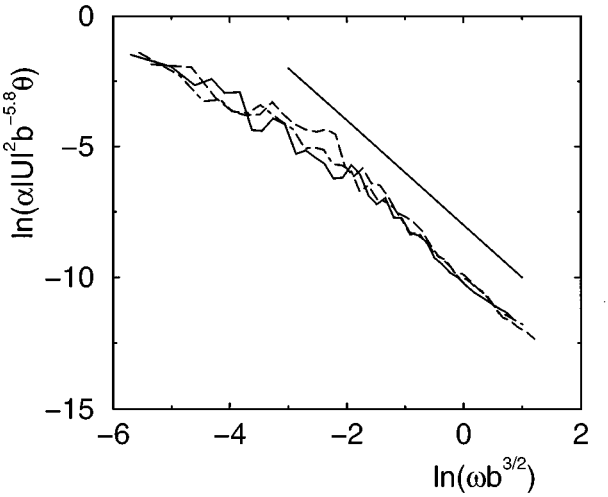

FIG. 8. The Fourier spectrum $\langle|U(\omega)|^2\rangle$ for the cases $b=4$, 6, and 8. The solid curve with slope 2 is drawn for reference.

then been averaged over more than 150 realizations. The results for $b=4$, 6, and 8 are reported in Fig. 8 in a doubly logarithmic plot. The best data collapse is obtained by assuming that $\langle|U(\omega)|^2\rangle \simeq b^{\varsigma}$ with $\varsigma=5.8$. At ''high'' frequencies, $\langle|U(\omega)|^2\rangle$ exhibits a Lorentzian-type behavior, which turns, at low frequencies, into a weak divergence that reveals the presence of nontrivial long-time correlations. In fact, by invoking the Wiener-Kintchin theorem, the low-frequency tail in the spectrum of $\langle|U(\omega)|^2\rangle$ can be connected with the relaxation properties of $M(t)$ towards its asymptotic value M_∞. More precisely, the power-law convergence of the type $t^{-\beta}$ assumed in Eq. (18) implies a power-law divergence as $\omega^{-1+\beta}$, which is compatible with our data. However, the low-frequency cutoff due to the finite time of our simulations prevents drawing a definite statement about the presence of a truly power-law divergence. Nevertheless, we can, at least, determine the crossover frequency ω_c separating the two temporal regimes, which turns out to be $\omega_c \simeq 0.02/b^2$. Such a frequency is approximately 100 times smaller than the mean spacing between the energy levels of the eigenstates which effectively participate in the evolution of the wave packet. This observation can be taken as an indirect confirmation of the role played by the Mott states in the long-time evolution. As has already been recalled, Mott states have quite a specific structure: they appear in pairs and are characterized by two humps, a distance L apart. This leads to a quasidegeneracy of the order of $\Delta E \approx \exp(-L/l_\infty)$, where L is typically much larger than the localization length l_∞. Accordingly, over long-time scales, a few Mott states may dominate the packet dynamics.

For what concerns the scaling behavior of the spectrum $\langle|U(\omega)|^2\rangle$ with respect to b, the estimated exponent $\varsigma \approx 6.6$ is in perfect agreement with Eq. (24). Indeed, the relation between the spectral density (or power spectrum) and the variance of the signal $M(t)$, implies

$$[\Delta M(t)]^2 = \sum_{\omega} \langle|U(\omega)|^2\rangle = \sum_{\omega b^{3/2}} b^{5.8}\langle|U(\omega b^{3/2})|^2\rangle = b^{5.8}[\Delta M(t/b^2)]^2. \tag{25}$$

By comparing Eq. (25) with Eq. (24), one obtains $\delta \approx 1.1$, instead of the previous estimate $\delta=0.7$. Whether this difference implies that ensemble averages are different from temporal averages, or simply that they are affected by (very) different finite-b corrections, is not clear at the moment.

V. STEADY-STATE DISTRIBUTION

A. General discussion

As mentioned above, the localization of all eigenfunctions [see Eq. (4)] implies that for $t \gg t_D$ the quantum steady state $f(n,t) \equiv |c_n(t)|^2$ fluctuates around an average profile $f_s(n) = \langle f(n,t)\rangle$. As the effective number of eigenstates composing a single wave packet is finite, the average profile does depend on the disorder realization. However, in the limit $b \to \infty$, the number of statistically independent components diverges and sample-to-sample fluctuations are expected to vanish. In that limit, temporal and ensemble averages should coincide as long as the motion is ergodic.

On the basis of diagrammatic techniques, many results have been obtained for the steady-state distribution $f_s(x)$ in continuous 1D models with white noise potential (here, x denotes the position of the electron). In particular, an exponential decay $f_s(x) \sim \exp(-|x|/4l_m)$ has been predicted for the tails of $f_s(x)$ (l_m, being the mean free path) [24]. A subsequent more accurate analysis [38] revealed the presence of the prefactor $|x|^{-3/2}$. Both findings are included in the global expression derived in [39],

$$f_s(x) = \frac{\pi^2}{16 l_m}\int_0^\infty \eta \sinh(\pi\eta)\frac{(1+\eta^2)^2}{[1+ch(\pi\eta)]^2} \times \exp\left(-\frac{1+\eta^2}{4l_m}|x|\right) d\eta. \tag{26}$$

In fact, the above expression implies that, close to the origin, the spatial dependence is purely exponential,

$$f_s(x) \sim \exp(-|x|/l_m), \quad x \ll l_m \tag{27}$$

while the asymptotic decay is described by

$$f_s(x) \sim |x|^{-3/2}\exp(-|x|/4l_m), \quad x \gg 4l_m. \tag{28}$$

Therefore, the above two equations reveal that the decay rate $S(x) \equiv [\ln f_s(x)]'$ (the prime denotes the derivative with respect to the argument), changes by a factor of 4. One consequence of the nonpurely exponential behavior is that the average size of the saturated packet is two times smaller than the asymptotic localization length $\langle|x|\rangle = 2l_m$. It is interesting to notice also that the asymptotic dependence (28) is similar to that for the conductance of 1D samples of finite size [40] in the strong localized regime; in this case x is the ratio of the sample size with the localization length. As no analytical results are available for quasi-1D systems, in Sec. V B we shall compare our numerical results with the above expressions, by fitting the only free parameter l_m.

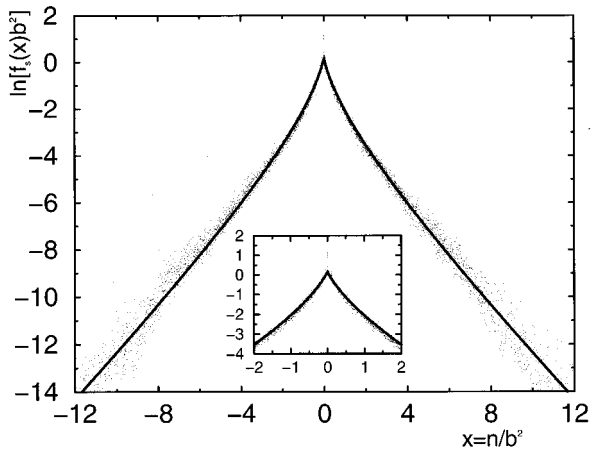

FIG. 9. Asymptotic average profile of the wave packet for $b=4\div 12$ after rescaling. The inset shows the behavior near to the maximum; smooth lines follow from the theoretical expression (26).

In any case, some information on the steady-state distribution $f_s(n)$ can be obtained from the structure of the eigenstates by exploiting the following equality:

$$f_s(n)=\sum_m |\varphi_m(n_0)\varphi_m(n)|^2, \tag{29}$$

where $\varphi_m(n)$ is the nth component of the eigenstate with energy E_m and n_0 is the position of the initial δ-like packet. Therefore, determining the asymptotic shape of a wave packet is tantamount to determining the average correlation properties of single eigenstates. Although no rigorous results are known in this direction, a phenomenological approach allowed us to shed some light on the closely related KR problem [6,30,32]. Because of the analogies between BRM and the KR, it is instructive to compare the results for the steady distribution as well. A rough estimation of the tails of $f_s(n)$ can be obtained in the following way (see [13,41] for details). If one assumes the simple exponential form $\varphi_m(n)\sim\exp(-|m-n|/l_\infty)$, for the mth eigenstate, Eq. (29) leads to the expression

$$f_s(n)\sim\exp\left(-\frac{2|n-n_0|}{l_\infty}\right), \tag{30}$$

which, in turn, implies $l_s=l_\infty$, where l_s is the localization length of the asymptotic packet [defined from the probability amplitude, i.e., taking the square root of Eq. (30)]. However, this result is inconsistent with the numerical data for the KR which instead indicate that $l_s\approx 2l_\infty$ [41]. To explain the latter result, it was suggested to take into account the large fluctuations of the eigenstates around their shape,

$$\varphi_m(n)\sim\frac{1}{\sqrt{l_\infty}}\exp\left(-\frac{|m-n|}{l_\infty}+\xi_{mn}\right), \tag{31}$$

where ξ_{mn} is a Gaussian noise with a zero mean and a variance [41],

$$\langle(\Delta\xi_{mn})^2\rangle=D_s|m-n|,\quad D_s\sim 1/l_\infty. \tag{32}$$

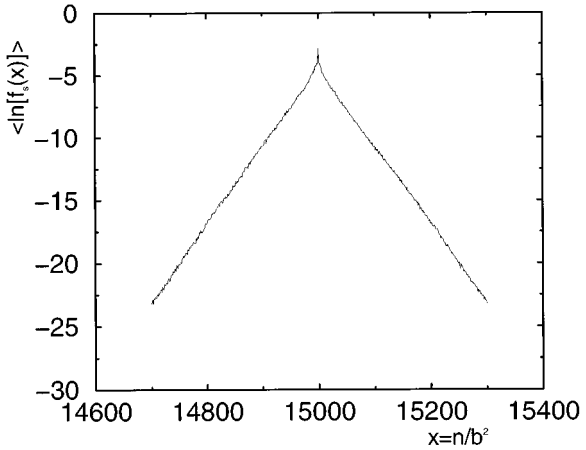

FIG. 10. Logarithm of the steady state f_n for $b=5$.

By inserting the ansatz (31) in Eq. (29) and averaging over the noise term, it was found that

$$\langle|\varphi_m(n)|\rangle\sim\exp\left(-\frac{|n-m|}{2l_\infty}\right), \tag{33}$$

implying that the linear average yields a different localization length compared to Eq. (30).

By repeating the same calculations for the expression (29), one obtains that $f_s\simeq\exp(|n-n_0|/l_\infty)$, which is found to be in agreement with the numerical results for the KR model as it implies $l_s=2l_\infty$.

However, relation (29) implies that the average $\langle|\phi_m(n)|^2\rangle$ should be used rather than $\langle|\phi_m(n)|\rangle$. In such a case, the result is

$$\langle|\varphi_m(n)|^2\rangle\sim\exp\left(-\frac{|n-m|}{2l_\infty}\right), \tag{34}$$

which implies that $f_s\simeq\exp(|n-n_0|/2l_\infty)$. The correctness of this expression is confirmed by the relation $l_s=4l_\infty$ that it implies.

B. Numerical data

In order to determine the asymptotic shape of the wave packet, we have followed the evolution of an initially δ-like packet for times $t\geqslant 120t_D$. The distribution $f_s(n)$ has then been obtained by averaging over more than 150 realizations for several b values in the range $b=4$–12. The results are reported in Fig. 9 with the by now standard scaling hypothesis,

$$\tilde{f}_s(x)=b^2 f_s(n),\quad x=n/b^2, \tag{35}$$

that is once more confirmed by the good data collapse.

A peculiarity of all our simulations is that $f_s(n_0)$ is larger than the neighboring values by approximately a factor of 3. The reason for this apparent anomaly can be traced back to the specific δ-like shape of the initial packet [that implies Eq. (29)] and to the spatial random structure of the eigenvectors. Indeed, the latter assumption, together with the observation that only a finite number L of channels effectively contribute to the sum in Eq. (29), leads to

$$f_s(n_0) \approx L\langle \varphi^4(n_0)\rangle;$$

$$f_s(n \neq n_0) \approx L^2\langle \varphi^2(n)\rangle\langle \varphi^2(n)\rangle. \quad (36)$$

Since it is known that $\langle \varphi^4\rangle = 3/L$, while $\langle \varphi^2\rangle = 1/L$ for the eigenfunctions of matrices belonging to the Gaussian orthogonal ensemble [3], we obtain that $f_s(n_0)/f_s(n) = 3$ for n close to but different from n_0. This value of the ratio is in pretty good agreement with the above mentioned numerical estimate.

Moreover, the numerical results reported in Fig. 9 strongly suggest that the decay of $f_s(n)$ in the vicinity of n_0 is definitely faster than in the tails. Therefore, it is very tempting to compare this data with the theoretical dependence derived for 1D disordered models [Eq. (26)]. The best fit of the only free parameter gives $l_m \sim 0.29$; the corresponding curve is shown in Fig. 9 (see the solid line). The very good agreement between the numerical results and the analytical curve over a broad range of x values suggests that a properly modified theory to include the determination of the mean free path from first principles should be able to account for the asymptotic properties of packets in quasi-1D systems as well.

One should also notice that the dependence of the slope on the distance from the center n_0 of the packet is an entirely new feature with respect to the analogous problem in the KR [41,13], where no evidence of two distinct regions of localization has been found. The reason for this discrepancy is not clear: on the one hand it is possible that this reflects an actual difference between the two models, on the other hand, it is possible that the accuracy of the numerical data for the KR [41] is not enough to reveal this peculiarity in the associated profile $f_s(n)$.

A further difference is the variation of the localization length of the eigenstates with the energy in BRM [see Eq. (5)]. Far from the center of the packet, we expect that the decay is dominated by the longest localization length $l_\infty(0) = 2/3$ (in b^2 units). On the other hand, from Eq. (28), we find that $l_s = 8 l_m \approx 2.32$, which is only slightly smaller than $4 l_\infty(0) \approx 2.66$. Accordingly, the equality $l_s = 4 l_\infty$ found in the phenomenological theory for KR and explained by invoking the presence of strong fluctuations of the individual eigenstates [41] appears to also hold in the present case. The small deviation is presumably to be attributed to the not yet vanishing contributions of more localized eigenstates. Instead, if we average over all energies, we obtain $\langle l_\infty(E)\rangle = 0.5$ (in b^2 units) which results in a localization length $l_s = 4\langle l_\infty(E)\rangle = 2$ for the total wave function. Moreover, it is interesting to notice that a direct determination of l_s by fitting the profiles reported in Fig. 9 with a pure exponential law, yields $l_s \approx 2$: this means that the multiplicative correction $1/|x|^{3/2}$ in expression (28) is essential for a correct estimate of l_s, if the range of n/b^2 is not large enough.

A further more direct confirmation of the presence of strong fluctuations in the various eigenstates is obtained by determining the localization length $l_s^{(l)}$ of the asymptotic packet from the logarithmic average $[\langle \ln(f_s)\rangle]$ of the single packets. The resulting profile, reported in Fig. 10, yields $l_s^{(l)} \approx 1.3$ to be compared with the value $l_s \approx 2.32$, obtained from the arithmetic average. Interestingly enough, the ratio between the two lengths $l_s^{(l)}$ and l_s for the shape of saturated wave packet, is approximately equal to 2 as known for the single eigenstates (see the Sec. V A).

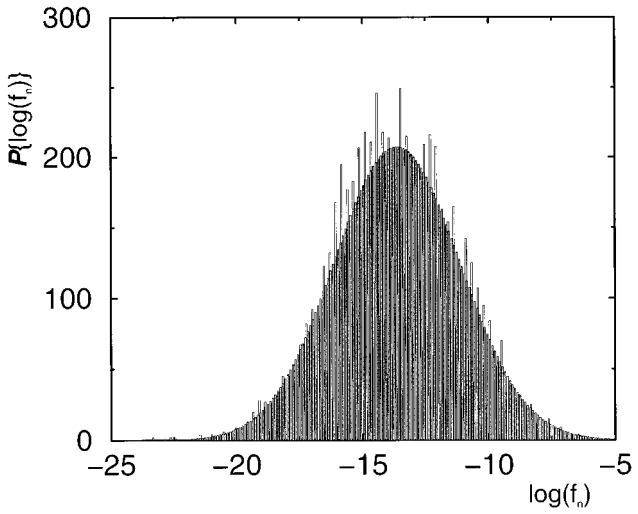

FIG. 11. Distribution of $\ln f_n$ for $b = 5$.

C. Fluctuations of the steady state

In this section we directly investigate the nature of wave-packet fluctuations in the asymptotic regime. This enables us to test the correctness of a conjecture relative to the single eigenvectors raised in the context of the KR. Indeed, fluctuations are very important in that they allow us to explain the difference between the decay rate of the wave packet and that of the eigenvectors.

Having in mind Eq. (31), we computed the logarithm of $f_s(n)$ and studied its variance at a distance $\Delta n = 6b^2$ from the center of the packet (averaging also over a small window of five neighboring sites, under the assumption that the fluctuations are nearly constant in such an interval). As a result, we have found that the distribution function of $y \equiv \ln(f_s)$ is, with a good accuracy, a Gaussian (see for instance the histogram reported in Fig. 11 which refers to the case $b = 5$ and is the result of 5000 simulations with independent realizations of the disorder). This represents a first confirmation that the hypotheses made in the KR can be profitably carried over to the present model.

More complete information is obtained by studying the fluctuations of y for different values of Δn. More precisely, we have computed the variance

$$\sigma^2(n) = \langle [\ln f_s(n)]^2\rangle - \langle \ln f_s(n)\rangle^2 \quad (37)$$

in the steady-state regime. The results for the cases $b = 5$–8 are reported in Fig. 12 with the scaling assumption $\sigma^2(n) = b^2\sigma^2(x)$, where $x \equiv \Delta n/b^2$. The data show that for large x, the variance grows linearly with x, indicating that the logarithm of the profile diffuses around the average value. This is a further confirmation of the validity of a relation of the type (31) for the wave packet and it is strengthened by the observation that the estimated slope is approximately equal to 1 in scaled units.

This behavior is also analogous to what happens in 1D disordered models, where it is assumed that the logarithm of

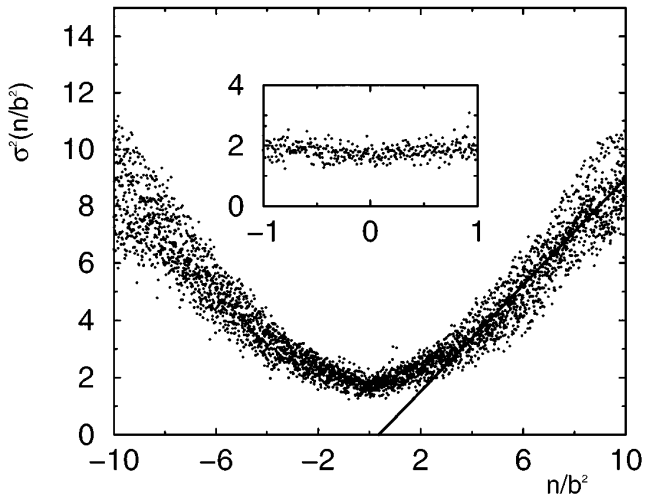

FIG. 12. Variance of $\ln f_n$ in the steady state after rescaling the x axis for $b=5,6,7,8,10$. The straight line is the fit for large values of x. The inset shows the behavior close to the maximum.

the absolute value of the Green's function $\ln|G(m,n;E)|$ has a Gaussian probability distribution with the mean equal to $-|m-n|/l_\infty$ and the variance equal to $|m-n|/l_\infty$ [42].

Another interesting observation concerns the central part of the packet (i.e., $|x|\leqslant 1$), where the variance σ^2 is almost constant, indicating that the amplitude values are essentially independent of one another (see also the inset in Fig. 12). Accordingly, all numerical findings do confirm the conjectures that have been so far utilized to present all the features of wave-packet diffusion in a coherent manner. Unfortunately, so far there are no analytical results concerning the structure of the eigenstates in the middle of their localization region, even in the well-studied 1D Anderson case.

VI. CONCLUSIONS

In the present paper we have studied the evolution properties of wave packets in quasi-1D disordered media described by tight-binding Hamiltonians with long-range random interactions. We have found that the wave packet: (i) first spreads ballistically, over a time scale of the order $t\sim 1/b^{1/2}$, which becomes negligible in the limit $b\to\infty$; (ii) exhibits a diffusive behavior, for times of the order $t\sim b^{3/2}$; (iii) finally, for times larger than $t_D\geqslant b^{3/2}$, stops spreading remaining asymptotically localized.

The scaling properties of the spread of the packet are different in the ballistic [see Eq. (10)] and diffusive [see Eq. (12)] regime. Beyond the ballistic regime, we propose the heuristic formula (18) to effectively describe both the diffusive spreading and the eventual saturation. The most interesting feature of Eq. (18) is the prediction of a power-law convergence of the wave packet width M to its asymptotic value, the deviation going to zero as $1/t^\beta$ with $\beta\simeq 0.9$. The parameter β accounts for the repulsion between those eigenstates which are effectively excited by the initial wave packet. More precisely, the slow convergence of M is attributed to the effect of Mott states, that are expected to eventually give rise to a logarithmic time dependence, that cannot be numerically observed.

The ''short''-time diffusive regime has been investigated by computing dM/dt when a small amount of time-dependent disorder was superimposed to the quenched disorder. As a result, we found that the diffusion coefficient in dimensionless units is approximately four times larger than the localization length, after averaging over the energy dependence. The presence of noise with strength g^2 of the order of a critical value $g_{\rm cr}^2\sim 1/b^3$, destroys quantum coherence and recovers classical diffusion.

Another issue addressed in this paper concerns the fluctuations of the size of the packet over different time scales. We found that in the diffusive regime, the relative amplitude of the fluctuations scales as $\mu\equiv\Delta M/M\sim 1/b^\eta$, where $\eta\simeq 0.9$. In the saturation regime, instead, we found conflicting results: ensemble averages suggest an anomalous scaling behavior, i.e., $\mu\sim 1/b^\delta$ with $\delta\simeq 0.7$ (in close agreement with the results for the KR); a frequency analysis suggest that $\delta\simeq 1.1$.

The study of the Fourier power spectrum shows that the tails of $|U(\omega)|^2$ have a Lorentzian-type form. At small frequencies, a weak singular behavior for $|U(\omega)|^2$ has been detected; this result is in agreement with the power-law convergence of M to its asymptotic value. Furthermore, we have been able to extract the crossover frequency ω_c, where deviations from $1/\omega^2$ start in $|U(\omega)|^2$. Such a frequency is two orders of magnitude smaller that the mean average separation between the energy levels which participate in the evolution of the wave packet. This is a further confirmation of the participation of Mott states to the long-time evolution.

For what concerns the asymptotic shape of the wave packets, we found that the scaling law (35) is well verified already for relatively large b values. Moreover, the analytic expression derived in the context of the 1D Anderson model [see Eq. (26)] reproduces pretty well the shape of the average profile, upon fitting a single parameter. A further interesting result of our numerical analysis concerns the difference by a factor of 4 between the decay rate of the asymptotic profile around the origin and that along the tails. Moreover, the difference between the localization length estimated from the average of the logarithm of the profile and that obtained from the linear average of the profile confirms the relevance of fluctuations. This observation is reinforced by the asymptotic linear growth of the variance σ^2 of the logarithm of the profile versus the distance from the center of the packet.

ACKNOWLEDGMENTS

We acknowledge useful discussions with B. Chirikov, Y. Fyodorov, A. Mirlin, S. Ruffo, and D. Shepelyansky. F.M.I is grateful to A. Bulgac for illuminating discussions of the related problems in nuclear physics application. T.K. and G.P.T. acknowledge discussions on the Anderson localization with C. Soukoulis and E. N. Economou. They also acknowledge partial support from Human Capital and Mobility Grant No. CHRXCT930331. T.K. acknowledges the support of Grant No. CHRX-CT93-0107 and also wishes to thank Instituto Nazionale di Ottica for the kind hospitality. Partial support by Grant No. INTAS-94-2058 is also acknowledged by F.M.I.

[1] *Statistical Theories of Spectra: Fluctuations*, edited by C.E. Porter (Academic, New York, 1965).
[2] M.L. Metha, *Random Matrices* (Academic, New York, 1967).
[3] T. Brody *et al.*, Rev. Mod. Phys. **53**, 385 (1981).
[4] O. Bohigas and M. Giannoni, in *Mathematical and Computational Methods in Nuclear Physics*, Vol. 209 of *Lecture Notes in Physics*, edited by J. S. Dehesa, J. M. G. Gomez, and A. Polls (Springer, Berlin, 1984), p. 1.
[5] G. Casati, B.V. Chirikov, J. Ford, and F.M. Izrailev, in *Stochastic Behavior in Classical and Quantum Hamiltonian Systems*, Vol. 93 of *Lecture Notes in Physics*, edited by G. Casati and J. Ford (Springer, Berlin, 1979), p. 334.
[6] F.M. Izrailev, Phys. Rep. **196**, 299 (1990).
[7] F. Haake, *Quantum Signatures of Chaos* (Springer, Berlin, 1991).
[8] G. Casati, I. Guarneri, F.M. Izrailev, and R. Scharf, Phys. Rev. Lett. **64**, 5 (1990).
[9] Y.V. Fyodorov and A.D. Mirlin, Int. J. Mod. Phys. **8**, 3795 (1994).
[10] F.M. Izrailev, Chaos Solitons Fractals **5**, 1219 (1995).
[11] E.P. Nachmedov, V.N. Prigodin, and U.A. Firsov, Zh. Éksp. Teor. Fiz. **92**, 2133 (1987) [Sov. Phys. JETP **65**, 1202 (1987)].
[12] B.V. Chirikov, F.M. Izrailev, and D.L. Shepelyansky, Sov. Sci. Rev. C **2**, 209 (1981).
[13] B.V. Chirikov, F.M. Izrailev, and D.L. Shepelyansky, Physica D **33**, 77 (1988).
[14] G. Casati and B. Chirikov, in *Quantum Chaos: Between Order and Disorder*, edited by G. Casati and B. Chirikov (Cambridge University Press, Cambridge, England, 1994).
[15] G. Casati and B. Chirikov, Physica D **86**, 220 (1995).
[16] T. Dittrich, Phys. Rep. **271**, 269 (1996).
[17] F.M. Izrailev, T. Kottos, A. Politi, S. Ruffo, and G. Tsironis, Europhys. Lett. **34**, 441 (1996).
[18] Y.V. Fyodorov and A.D. Mirlin, Phys. Rev. Lett. **67**, 2405 (1991).
[19] The only condition is that the amplitude of the matrix elements has to decrease sufficiently fast in such a way that the second moment of the envelope is finite [9,18].
[20] G. Casati, L. Molinari, and F.M. Izrailev, Phys. Rev. Lett. **64**, 1851 (1990).
[21] M.I. Molina and G.P. Tsironis, Phys. Rev. Lett. **73**, 464 (1994).
[22] P.W. Anderson, Phys. Rev. **109**, 1492 (1958).
[23] N.F. Mott and W.D. Twose, Adv. Phys. **10**, 107 (1961).
[24] V.L. Berezinskii, Zh. Éksp. Teor. Fiz. **65**, 1251 (1973) [Sov. Phys. JETP **38**, 620 (1974)].
[25] G. Casati, B.V. Chirikov, I. Guarneri, and D. Shepelyansky, Phys. Rep. **154**, 77 (1987).
[26] S. Fishman, D.R. Grempel, and R.E. Prange, Phys. Rev. Lett. **49**, 509 (1982).
[27] N. Mott, Philos. Mag. **22**, 7 (1970).
[28] N.F. Mott and E.A. Davis, *Electronic Processes in Non-Crystalline Materials* (Oxford, New York, 1971).
[29] L.P. Gor'kov, O.N. Dorokhov, and F.V. Prigara, Zh. Éksp. Teor. Fiz. **84**, 1440 (1983) [Sov. Phys. JETP **57**, 838 (1983)]; **85**, 1470 (1983) [**58**, 852 (1983)].
[30] D. Cohen, Phys. Rev. A **44**, 2292 (1991).
[31] B.V. Chirikov, Chaos **1**, 95 (1991).
[32] G.P. Berman and F.M. Izrailev, Institute of Physics Report No. 497-f, 1988 (unpublished).
[33] T. Dittrich and U. Smilansky, Nonlinearity **4**, 59 (1991); **4**, 85 (1991).
[34] A. Bulgac, D. Kusnezov, and G. Do Dang, Ann. Phys. (Leipzig) **242**, 1 (1995); Phys. Rep. **264**, 67 (1966); in *Recent Progress in Many Body Theories*, edited by E. Schachinger, H. Mitter, and H. Sormann (Publisher, City, 1995), Vol. 4, p. 293.
[35] E. Ott, T.M. Antonsen, Jr., and J.D. Hanson, Phys. Rev. Lett. **53**, 2187 (1984).
[36] T. Dittrich and R. Graham, Ann. Phys. (N.Y.) **200**, 363 (1990).
[37] G. Casati, B.V. Chirikov, and F.M. Izrailev (unpublished).
[38] A.A. Gogolin, V.I. Melnikov, and E.L. Rashba, Zh. Éksp. Teor. Fiz. **69**, 327 (1975) [Sov. Phys. JETP **42**, 168 (1976)].
[39] A.A. Gogolin, Zh. Éksp. Teor. Fiz. **71**, 1912 (1976) [Sov. Phys. JETP **44**, 1003 (1976)].
[40] M.R. Zirnbauer, Phy. Rev. Lett. **69**, 1584 (1992).
[41] B.V. Chirikov and D.L. Shepelyansky, Radiofiz. **29**, 1041 (1986).
[42] E.N. Economou, in *Green's Functions in Quantum Physics*, Vol. 7 of *Solid State Physics*, edited by M. Cardona, P. Fulde, K. von Klitzing, and H.-S. Queisser (Springer-Verlag, Berlin, 1979).